Languages | IPCC web pages | [ ] Search

© ® The Nobel Foundation

IPCC honoured with the 2007 Nobel Peace Prize

IPCC
Phone: +41-22-730-8208/84
e-mail: IPCC-Sec@wmo.int

REPORTS - SPECIAL REPORTS

Aviation and the Global Atmosphere

Table of contents [ ]

Other reports in this collection

3.2.3. Soot and Metal Particles

3.2.3.1. Soot

Aircraft jet engines directly emit solid soot particles. Soot encompasses all primary, carbon-containing products from incomplete combustion processes in the engine. Besides the pure (optically black) carbon fraction, these products may also contain nonvolatile (gray) organic compounds (e.g., Burtscher, 1992; Bockhorn, 1994). Soot parameters of importance for understanding plume processes are concentration and size distribution at the engine exit, nucleating and chemical properties, and freezing ability. Soot emissions for current aircraft engines are specified under the International Civil Aviation Organization (ICAO) using smoke number measurements (Chapter 7). The smoke number is dominated by the largest soot particles collected onto a filter. Sampling soot particles smaller than about 300 nm on such filters becomes inefficient. Correlations between smoke number and soot mass concentrations (e.g., Champagne, 1988) are used to estimate the soot mass EI from ICAO certification data. A mean value has been estimated to be approximately 0.04 g/kg fuel for the present fleet (D�pelheuer, 1997). Because soot emissions depend strongly on engine types, power settings, and flight levels, additional information is generally needed to relate smoke number to emissions under flight conditions. However, details of the size distribution and physicochemical properties of soot under flight conditions are generally not known and cannot be inferred from smoke number data. Soot particle measurements for a variety of contemporary engines show values that scatter around 1015/kg fuel (Figure 3-3b). Thus, soot is about 100 times less abundant in the plume than volatile aerosol particles; no significant, if any, dependence exists between soot and fuel sulfur content (Petzold et al., 1997, 1999; Anderson et al., 1998a; Paladino et al., 1998). Values of 1014 to 1015/kg fuel are consistent with a mass range of 0.01 to 0.2 g/kg fuel for individual engines using estimated size distributions. The older Concorde and T-38 engines show exceptionally high number EIs, whereas one modern subsonic engine emits much fewer soot particles (about 1013/kg fuel) (Howard et al., 1996). Soot particles are composed of individual, nearly spherical particles (spherules), which have a number mean radius between 10 and 30 nm and exceed the size of volatile aerosol particles in a young plume (Hagen et al., 1992; Rickey, 1995) (Figure 3-2). Several spherical soot particles may aggregate and form a complex chain structure that may change with time (Goldberg, 1985). The smallest soot particles will be most rapidly immersed in background aerosol droplets by coagulation, consistent with the fact that only larger individual soot particles or agglomerates with radii larger than about 50 to 100 nm are observable at cruising levels (Sheridan et al., 1994). Reported estimates of soot surface area at the engine exit are in the range of 5,000 to 105 $\mu m^2 cm^{-3}$ (Rickey, 1995; Petzold et al., 1999). These values continually decrease as the plume dilutes.

Much less information is available concerning the hydration properties of exhaust soot. In the initial stages of formation, graphite-like soot particles are hydrophobic. However, laboratory observations have shown that n-hexane soot particles and other black carbons are partially hydrated (e.g., Chughtai et al., 1996). Soot particles fresh from jet engines very likely become hydrophilic by oxidation processes or deposition of water-soluble species present in the exhaust. Irregular surface features and chemically active sites can also increase chemical reactivity and amplify heterogeneous nucleation processes.

A clear correlation between fuel sulfur content and soluble mass fractions found on fresh exhaust soot suggests that soot hydrates more effectively with increasing EI(S) and that H_2SO_4 is the primary soluble constituent (Whitefield et al., 1993). Hydration of carbon particles was observed under water-subsaturated conditions after treatment with gaseous H_2SO_4 (Wyslouzil et al., 1994). This increase in H_2O adsorption is in qualitative agreement with an analysis of the wetting behavior of graphitic carbon under plume conditions (K�rcher et al., 1996b). Heterogeneous nucleation of H_2SO_4 hydrates on soot was found to be unlikely under plume conditions. Soot hydration properties may also change after treatment with OH and ozone (K�rcher et al., 1996b; Kotzick et al., 1997).

Production of water-soluble material by the interaction of soot with SO_2 is unlikely because the sticking probabilities of gaseous SO_2 on amorphous carbon are too small (Andronache and Chameides, 1997; Rogaski et al., 1997). However, SO_3 and H_2SO_4 might easily adsorb on soot prior to volatile particle formation and may explain measured soluble mass fractions on soot (K�rcher, 1998b). Sulfur may also become incorporated into soot already within the engines, possibly via S-containing hydrocarbons involved in soot formation (Petzold and Schr�der, 1998). Scavenging of small volatile droplets constitutes another soot activation pathway (Zhao and Turco, 1995; Brown et al., 1996b; Schumann et al., 1996). The resulting liquid H_2SO_4/H_2O coating increases with plume age and may enhance the ice-forming ability of soot, which is only poorly known (Section 3.2.4), or it may suppress reactions identified in the laboratory using dry soot surfaces (Gao et al., 1998).

3.2.3.2 Metal Particles

Aircraft jet engines also directly emit metal particles. Their sources include engine erosion and the combustion of fuel containing trace metal impurities or metal particles that enter the exhaust with the fuel (Chapter 7). Metal particles-comprising elements such as Al, Ti, Cr, Fe, Ni, and Ba-are estimated to be present at the parts per billion by volume (ppbv) level at nozzle exit planes (CIAP, 1975; Fordyce and Sheibley, 1975). The corresponding concentrations of 10^7 to 10^8 particles/kg fuel (assuming 1-mm radius; see below) are much smaller than for soot. Although metals have been found as residuals in cirrus and contrail ice particles (Chen et al., 1998; Petzold et al., 1998; Twohy and Gandrud, 1998), their number and associated mass are considered too small to affect the formation or properties of more abundant volatile and soot plume aerosol particles.

3.2.4. Contrail and Ice Particle Formation

3.2.4.1. Formation Conditions and Observations

Contrails consist of ice particles that mainly nucleate on exhaust soot and volatile plume aerosol particles. Contrail formation is caused by the increase in relative humidity (RH) that occurs in the engine plume as a result of mixing of warm and moist exhaust gases with colder and less humid ambient air (Schmidt, 1941; Appleman, 1953). The RH with respect to liquid water must reach 100% in the young plume behind the aircraft for contrail formation to occur (H�hndorf, 1941; Appleman, 1953; Busen and Schumann, 1995; Jensen et al., 1998a). The thermodynamic relation for formation depends on pressure, temperature, and RH at a given flight level; fuel combustion properties in terms of the emission index of H_2O and combustion heat; and overall efficiency h (Cumpsty, 1997). h, defined as the fraction of fuel combustion heat that is used to propel the aircraft, can be computed from engine and aircraft properties (Schumann, 1996a; see also Section 3.7). Only the fraction (1-h) of the combustion heat leaves the engine with the exhaust gases. As the value of h increases, exhaust plume temperatures decrease for a given concentration of emitted water vapor, hence contrails form at higher ambient temperatures and over a larger range of altitudes in the atmosphere (Schmidt, 1941). Several recent studies reported formation and visibility of contrails at temperatures and humidities as predicted by

thermodynamic theory for a variety of aircraft and ambient conditions (Busen and Schumann, 1995; Schumann, 1996b; Schumann et al., 1996; Jensen et al., 1998a; Petzold et al., 1998). These data are compiled in Figure 3-4. The mixing process in the expanding exhaust plume is close to isobaric, so the specific excess enthalpy and water content of the plume decrease with a fixed ratio as plume species dilute from engine exit to ambient values. Hence, plume conditions follow straight "mixing lines" in a plot of H_2O partial pressures versus temperature (Schmidt, 1941) (Figure 3-4). The thermodynamic properties of H_2O are such that the saturation pressures over liquid water and water-ice (solid and dashed lines) increase exponentially with temperature. Therefore, within the first second in the plume, the exhaust RH increases to a maximum, then decreases to ambient values. The ambient temperature reaches threshold values for contrail formation when the mixing lines touch the liquid saturation curve in Figure 3-4b. Contrails persist when mixing-line endpoints fall between the liquid and ice saturation pressures-that is, when the ambient atmosphere is ice-supersaturated. Without ambient ice supersaturation, contrail ice crystals evaporate on time scales of seconds to minutes. Short-lived contrails may also form without ambient water vapor if ambient temperatures are sufficiently low.

Contrails become visible within roughly a wingspan distance behind the aircraft, implying that the ice particles form and grow large enough to become visible within the first tenths of a second of plume age. Ice size distributions peak typically at 0.5 to 1 �m number mean radius (Figure 3-2). A lower limit concentration of about 104 cm^{-3} of ice-forming particles in the plume (at plume ages between 0.1 and 0.3 s) is necessary for a contrail to have an optical depth above the visibility threshold (K�rcher et al., 1996b). These values and the corresponding mean radii of 1 �m of contrail ice particles are in agreement with in situ measurements in young plumes (Petzold et al., 1997). Initial ice particle number densities increase from 104 to 105 cm^{-3} and mean radii decrease from 1 to 0.3 �m when the ambient temperature is lowered by 10 K from a typical threshold value of 222 K (K�rcher et al., 1998a). Although aerosol and ice particle formation in a contrail are influenced by the fuel sulfur content (Andronache and Chameides, 1997, 1998), it has only a small (< 0.4 K) impact on the threshold temperature for contrail formation (Busen and Schumann, 1995; Schumann et al., 1996). Simulations of contrail formation further suggest that contrails would also form without soot and sulfur emissions by activation and freezing of background particles (Jensen et al., 1998b; K�rcher et al., 1998a). However, the resulting contrails would have fewer and larger particles.

Ice particle size spectra within and at the edge of young contrails systematically differ from each other (Petzold et al., 1997). Ambient aerosol may play a larger role in contrail regions that nucleate at the plume edges, where the ratio of ambient to soot particles is largest and when ambient temperatures are low (212 K) (Jensen et al., 1998b). Ice particles may also nucleate on ambient droplets in the upwelling limbs of vortices and could contribute to contrail ice mass (Gierens and Str�m, 1998). Metal (and soot) particles have been found as inclusions in contrail ice particles larger than 2 to 3 �m in radius (Twohy and Gandrud, 1998), but these particles are numerically unimportant compared with other plume particles. Contrail ice crystals evaporate quickly when the ambient air is subsaturated with respect to ice, unless the particles are coated with other species such as HNO_3 (Diehl and Mitra, 1998). Simulations suggest that a few monolayers of HNO_3 may condense onto ice particle surfaces and form NAT particles in stratospheric contrails (K�rcher, 1996). These particles would be thermodynamically stable and longer lived and would cause a different chemical perturbation than would short-lived stratospheric contrails composed of water ice. However, the relevance of this effect on larger scales has not yet been studied because no parameterization of NAT particle nucleation in aircraft plumes exists for use in atmospheric models (Chapter 4).

Figure 3-4: *Water vapor partial pressure and temperature measurements and calculations from various contrail studies.*

3.2.4.2. Freezing of Contrail Particles

In a young contrail, activated particles first grow to sizes > 0.1 �m by water uptake before many of them freeze homogeneously to form water-ice particles (K�rcher et al., 1995; Brown et al., 1997). The fraction of H_2SO_4/H_2O droplets that freezes depends on the actual droplet composition, which affects the homogeneous freezing rate, the time evolution of H_2O supersaturation and temperature in the plume, and possible competition with heterogeneous freezing processes involving soot (see Figure 3-1). Pure water droplets freeze homogeneously (without the presence of a foreign substrate) at a rate that grows in proportion to droplet volume and becomes very large when the droplet is cooled to the homogeneous freezing limit near about -45�C (Pruppacher, 1995). Acidic solutions freeze at lower temperatures than pure water. Freezing is often induced heterogeneously by solid material immersed inside a droplet (immersion freezing) or in contact with its surface (contact freezing). Prediction of heterogeneous freezing rates requires detailed knowledge about the ice-forming properties of droplet inclusions (Pruppacher and Klett, 1997). If homogeneous and heterogeneous freezing processes are possible, the most efficient freezing mode takes up available H_2O and may prevent the growth of other particle modes.

When the ambient temperature is near the threshold value for contrail formation, models suggest that volatile aerosol particles take up only a little water and stay below the critical size (radii > 2 to 5 nm) required for growth and subsequent freezing (K�rcher et al., 1995). This critical size-hence freezing probability-depends on maximum supercooling reached in the expanding plume. Particle growth rates-hence freezing rates-are larger in cooler and more humid ambient air, so volatile particles may contribute considerably to ice crystal nucleation at temperatures below the contrail threshold value. This result is supported by observations of contrails and their microphysical properties for different fuel sulfur levels (Petzold et al., 1997) and environmental temperatures (Freudenthaler et al., 1996). Volatile particles grown on charged droplets are more easily activated than neutral mode droplets (compare in Figure 3-2), therefore may play an enhanced role in contrail formation (Yu and Turco, 1998b). Ambient particles also contribute to ice crystal nucleation in the contrail (Twohy and Gandrud, 1998).

In contrail particle formation, heterogeneous freezing processes involving soot (see Figures 3-1 and 3-5) compete with homogeneous freezing of volatile plume
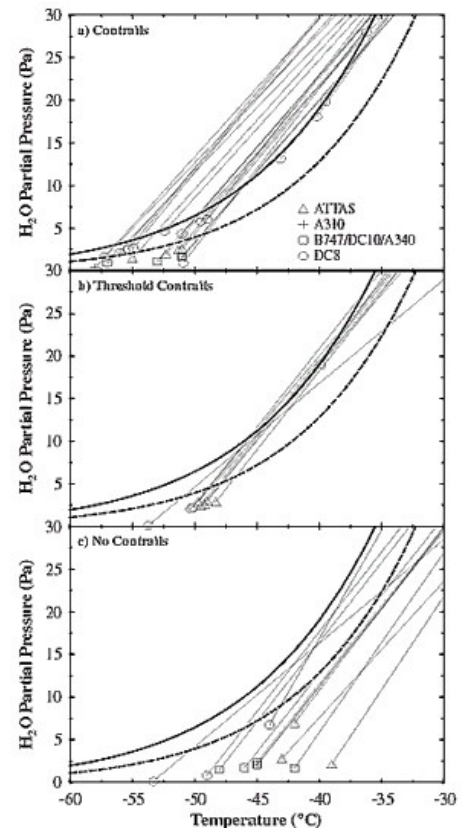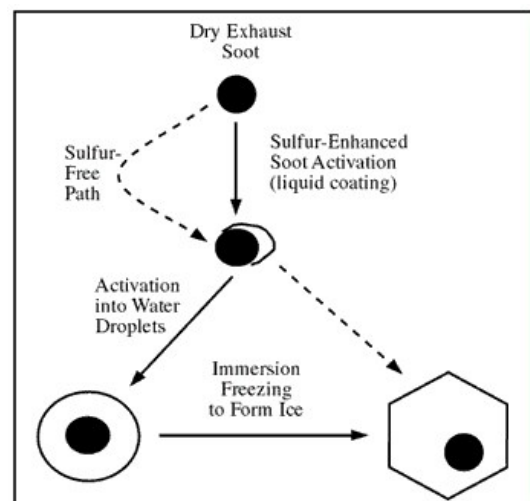
particles. Volatile droplets will be prevented from freezing if rapid freezing of soot-containing particles occurs. Although this analysis is supported by model simulations and some observations (Gierens and Schumann, 1996; K�rcher et al., 1996b, 1998a; Schumann et al., 1996; Brown et al., 1997; Konopka and Vogelsberger, 1997; Schr�der et al., 1998a; Twohy and Gandrud, 1998), the freezing probability of soot is poorly known because unique evidence that soot is directly involved in ice formation is difficult to obtain from in situ measurements. On the other hand, fresh soot particles do not act as efficient ice (deposition) nuclei in the exhaust (Rogers et al., 1998), consistent with the absence of contrails at temperatures above the liquid water saturation threshold.

Figure 3-5: Soot activation and heterogeneous freezing in young aircraft exhaust plumes (K�rcher, 1998a).

Contrails observed near threshold formation conditions are thought to result from freezing of water on soot particles (K�rcher et al., 1996b; Schumann et al., 1996; Brown et al., 1997) (Figure 3-5). This result is supported by laboratory experiments (DeMott, 1990; Diehl and Mitra, 1998) that provide evidence that soot may induce ice formation by heterogeneous immersion freezing at temperatures colder than about 250 K. Water activation of soot may result from the formation of at least a partial surface coating of H_2SO_4/H_2O droplets, which likely develops for average to high fuel sulfur levels (Figure 3-5). Hence, more fuel sulfur leads to a greater number of ice particles. However, observations demonstrate that the number of ice particles (diameter > 300 nm) in young contrails increases by only about 30% when the fuel content increases from 6 to 2700 ppm (Petzold et al., 1997), as model simulations of contrail formation also show (K�rcher et al., 1998a).

Contrails at threshold conditions appear to be formed for very low (2 ppm) fuel sulfur content in the same manner as for average fuel sulfur content (260 ppm) (Busen and Schumann, 1995), but their properties differ measurably for larger fuel sulfur content (Schumann et al., 1996). This result suggests that soot may take up water even at zero fuel sulfur content, though this uptake may be enhanced in the presence of sulfur emissions (K�rcher et al., 1998a; see Figure 3-5).

The presence of liquid coatings may alter the chemical reactivity of dry exhaust soot, which is poorly known (Chapter 2). Soot particles acting as freezing nuclei have the potential to alter cirrus cloud properties (see Section 3.4). Present observations do not rule out the possibility that aircraft soot particles can act as freezing nuclei in cirrus formation, perhaps even without a H_2SO_4/H_2O coating. Information is lacking on how the chemical reactivity and freezing properties of soot might change in aging plumes from interactions with background gases and particles or as a result of aerosol processing in contrails.

Table 3-2: Emission indices and estimated global emission rates of exhaust products of the present (1992) aircraft fleet using representative emission indices. Emission sources other than aircraft and estimated magnitudes of these emissions are listed in the last two columns. Values in parentheses indicate estimated range (adapted from Fabian and K�rcher, 1997; Schumann, 1994).

Fuel and Emissions	Emission Index (g pollutant/kg fuel)	Emission Rate (1992 fleet) (Tg yr^{-1})	Comparable Emission (Tg yr^{-1})	Comparable Emission Source
Fuel	-	140 (139-170)a	3140	Total consumption of petrol
H_2O	1260	176	45	CH_4 oxidation in the stratosphere
			525000	Evaporation from Earth's surface
NO_x (as NO_2)	14 (12-16)a	2	2.9 � 1.4	Flux from the stratosphere
			90 � 35	All anthropogenic sources
Soot burning	0.04 (0.01-0.1)b	0.006	12c	Fossil fuel combustion and biomass
Sulfur	0.4 (0.3-0.5)	0.06	65d	Total from fossil fuel combustion
			10-50	Natural source, mostly as DMSe
			2.7f	Non-eruptive volcanoes
			4.0g	Eruptive volcanoes
C_xH_y surface	0.6 (0.2-3.0)	0.1	90	Anthropogenic emissions at Earth's

a) From Chapter 9.
b) D�pelheuer, 1997.
c) Liousse et al., 1996.
d) Benkovitz et al., 1996.
e) Watson et al., 1992.
f) Spiro et al., 1992.
g) Chin et al., 1996.